Appl Biochem Biotechnol (2017) 181:379–390
DOI 10.1007/s12010-016-2218-1

Anti-Metastatic and Anti-Invasion Effects of a Specific Anti-MUC18 scFv Antibody on Breast Cancer Cells

Mozafar Mohammadi[1,2] · **Foroogh Nejatollahi**[2,3] · **Younes Ghasemi**[1,4] · **Sayyid Nooreddin Faraji**[1,2]

Received: 21 April 2016 / Accepted: 15 August 2016 /
Published online: 27 August 2016

Abstract Breast cancer is the most common malignancy in women. Altered expression of MUC18, a cell surface receptor, and its interaction with Wnt-5a as its ligand, affects the motility and invasiveness of breast cancer cells. In this study, we explored the Wnt-5a binding site and designed an antigenic epitope on the MUC18 receptor using in silico methods. A specific single-chain variable fragment (scFv) was isolated against the epitope by several panning processes. The binding ability of the scFv to the related epitope was evaluated in ELISA and flow cytometry. The inhibitory effects of the selected scFv on MUC18 positive cell line, MDA-MB231, was assessed by migration and invasion assays. The results demonstrated isolation of specific scFv with frequency of 40 % which showed significant binding with the epitope in both ELISA and fluorescence-activated cell sorting (FACS) analyses. The antibody inhibited the migration (76 %) and invasion (67 %) of MUC18 positive cell line. The results suggest the specific anti-MUC18 scFv as an effective antibody for breast cancer immunotherapy.

Keywords MUC18 · Wnt-5a · scFv · Metastases · Molecular modeling · Protein docking

✉ Foroogh Nejatollahi
nejatollaf@sums.ac.ir

[1] Faculty of advanced medical sciences and technologies, Shiraz University of Medical Sciences, Shiraz, Iran

[2] Recombinant antibody laboratory, Dept. of immunology, Shiraz University of Medical Sciences, Shiraz, Iran

[3] Shiraz HIV/AIDS research center, Shiraz University of Medical Sciences, Shiraz, Iran

[4] Department of Pharmaceutical Biotechnology; School of Pharmacy, Shiraz University of Medical Sciences, Shiraz, Iran

Introduction

The formation of secondary tumors due to metastasis of cancer cells to distal organs is the primary cause of death in women with breast cancer [11]. Evidences show that malignant cells in breast cancer undergo an epithelial to mesenchymal transition (EMT) state. This change enables them to become motile, especially in the ER−/PR−/HER2−triple-negative breast cancer (TNBC) which is the most aggressive and lethal type of breast cancer [22]. MUC18 or CD146 is a cell surface receptor which is also known as melanoma cell adhesion molecule or MCAM. It has been shown that the altered expression of MUC18 affects the motility and invasiveness of many epithelial tumors such as breast cancer cells in vitro and metastasis in vivo. MUC18 may also play an important role in awakening the dormant metastatic tumor cells to enter into an aggressive growth state [31]. MUC18 is a glycoprotein with a typical single-spanning transmembrane structure. It is composed of 646 amino acids, including an N-terminal extracellular domain with 558 residues, which comprises five immunoglobulin-like domains (V1-V2-C2-C2-C2) [15, 16, 32]. Wnt-5a which has been implicated in oncogenesis and in several developmental processes is an extracellular ligand for MUC18. One of the mechanisms of cell migration is through MUC18 and Wnt-5a interaction, into which Wnt-5a promotes cell migration and invasion by recruitment of MUC18 receptor; this is required for actomyosin contraction [30]. After attachment of Wnt-5a to MUC18, Wnt5a-induced activation of Dishevelled (Dvl) and c-Jun amino-terminal kinase (JNK) happens in tumor cell cytoplasm. The interaction between cytoplasmic tail of MUC18 and Dvl2 protein promotes cell migration and facilitate the movement of tumor cell to other tissues. These evidences suggest a model into which MUC18 acts as a canonical Wnt5a receptor in regulating cell migration and invasion [33].

ScFvs (single chain fragment variables) have been shown as an alternative choice to full-length monoclonal antibodies (mAbs) in therapeutic applications [25, 27]. ScFvs are composed of variable heavy (VH) and variable light (VL) domains that are joined by a peptide linker. They display improved pharmacokinetic properties. These molecules can penetrate more rapidly into solid tumors as compared to full-length antibodies [6, 23, 26]. Lacking the Fc region in recombinant antibodies, provides their low immunogenicity, and making them as better therapeutic agents compared to intact mAbs in many applications [21, 24].

In this study, an immunodominant epitope was determined on MUC18 receptor by evaluation of its interaction with Wnt-5a (as ligand) using in silico methods. Afterward, a specific scFv against the epitope was isolated and its inhibition properties on breast cancer cell migration and invasion were assessed in vitro.

Materials and Methods

Epitope Designing by In silico Techniques

The 3D model of MUC18 and Wnt-5a molecules was made by employing homology modeling using Phyre2 [13] and SWISS MODEL [3, 4, 8, 14] servers, respectively. The simulated structures were evaluated by the SAVES [1] program. Subsequently, to investigate the interaction of Wnt-5a and CD146, protein docking was done using Hex 8.0.0 program [18]. To find the antigenic epitope on CD146 molecule EpiC, antigenicity and functional prediction server [9] was used. All visualizations were done by Chimera software [28].

Selection of Anti-MUC-18 scFv

The panning process was performed as follows: Nunc-immunotubes were coated with the 100 μg/ml antigenic peptide. Tubes were blocked with 2 % skimmed milk and incubated at 37 °C for 2 h, then washed with PBS/Tween-20. Phage rescue supernatant, 10^{10} to 10^{11} phages in blocking solution [7], were added to immune tubes and incubated at room temperature. The TG-1 culture was added to the tubes and incubated to allow bacterial cells become infected by the phages. Infected TG-1 bacteria were collected by centrifugation. Four rounds of panning were carried out to select scFvs with high affinity and high specificity against the MUC18 epitope.

PCR and DNA Fingerprinting

To determine the common patterns with high frequency, PCR and DNA fingerprinting of randomly selected clones were done after the fourth round of panning. After checking the insert size with PCR, 17 μl of each PCR product was mixed with 2 μl of restriction enzyme buffer and 1 μl of frequent-cutting Mva I restriction enzyme (Fermentas, Lithuania) and digested at 37 °C for 2 h. The samples were run on a 2.5 % agarose gel.

Enzyme-Linked Immunosorbent Assay

Ninety-six well polystyrene plates (NUNC™, Denmark) were coated with 100 μg/ml peptide in order to perform the phage ELISA assay. The wells were blocked with 2 % skimmed milk and incubated at 37 °C for 2 h. After washing three times with PBS/Tween-20 and three times with PBS, phage antibodies were added to each well and incubated at room temperature for 2 h. Following washing, the plate was incubated with rabbit anti-Fd bacteriophage antibody (Sigma, USA) for 1 h. Finally, the plate was washed and incubated with goat HRP conjugated anti-rabbit IgG (Sigma, USA) for 1 h at 37 °C. After adding the substrate (TMB) and H2SO4 as stop solution, the absorbance was measured by ELISA reader at 450 nm.

FACS Analysis of the Phage scFv

Cell surface binding capacities of selected phage scFvs were determined by flow cytometry. Briefly, 5×10^5 MDA-MB 231 (MUC18-positive) and SKBR3 (MUC18-negative) cell lines were treated with 10^{10} phage scFv, incubated for 35 min in the dark place at 4 °C and washed three times with cold media. 1/500 dilution of rabbit anti-fd antibody was added and incubated at room temperature for 40 min. The cells were washed three times with cold media and incubated with 1/500 dilution of goat PE-conjugated anti-rabbit antibody (Sigma) at room temperature for 30 min. The number of bounded phage scFvs was measured by a fluorescence-activated cell sorting (FACS) Calibur (BD biosciences, USA).

Expression and Extraction of Soluble scFv

Log-phase *Escherichia coli* HB2151 cells were infected with the selected phage clone for 30 min at 37 °C without shaking followed by 30 min with shaking. The infected cells were plated on 2TYG plate containing 100 μg/ml ampicillin. Single colonies were grown in 5 mL of 2TY medium overnight at 30 °C with shaking, diluted with 50 mL of fresh 2TY medium

incubation at 30 °C with shaking for further 1 h. After centrifugation, the pellet was suspended in 50-ml 2TY including 1-mM IPTG and incubated overnight at 30 °C with shaking to induce the expression of soluble scFvs. Bacterial culture was centrifuged and cell pellets were suspended in 0.5 ml of 1 M ice-cold TES (0.2 mol/L Tris-HCl, pH 8.0, 0.5 mmol/L EDTA, 0.5 mol/L sucrose) followed by adding 0.75 ml of 1/5 M TES. After incubation for 30 min on ice, the supernatant containing the periplasmatic fraction was centrifuged and stored at −20 °C.

SDS-PAGE and Western Blot Analysis

Solubilized scFvs were loaded onto a 12 % SDS gel and electrophoresed by SDS-PAGE. Afterward, the protein bands were electro blotted onto PVDF membrane. The PVDF paper was blocked with 5 % skimmed milk in PBS/0.5 % Tween overnight at 4 °C and washed five times with PBS/0.5 % Tween. The mouse anti-c-myc tag HRP conjugated antibodies (Abcam) were used at concentration 1/10,000 in blocking solution and incubated with the membrane for 2 h at room temperature with shaking. Afterward, the membrane washed five times with PBS/0.5 % Tween. After washing, the ECL was used as a chemiluminescence reagent and images were taken by the ChemiDoc™ MP Imaging system (Bio-Rad, USA).

Wound Healing Assay

Wound healing experiments were done for checking tumor cell migration. Briefly, MB-231 cells were seeded at a density of 10^6 in six well culture plate. After reaching to 100 % confluence, cells were scratched with a 10-μL tip to make an artificial wound. Wounded cell layers were treated with or without 1 μg/ml of anti-MUC18 scFv. Wound closure was monitored with an inverted microscope (Micros, Austria) by taking pictures of the same section at 0, 4, 6, and 8 h after intervention. Wound area was measured using Digimizer software (Medcalc software, Mariakelke, Belgium) and calculated as the amount of wound closure from time point $t = 0$.

Cell Migration Analysis

MDA-MB231 cells were trypsinized and suspended in FBS-free RPMI-1640 medium. A total of 5×10^4 cells in 100 μl of FBS-free medium containing 1 μg/ml of anti-MUC18 scFv were seeded into the top chamber of the transwell with a non-coated polycarbonate membrane (6.5-mm diameter insert, 8.0-μm pore size; BD Biosciences, San Jose, CA, USA). 600-μl RPMI-1640 medium supplemented with 10 % FBS was added to the lower chamber as a chemo-attractant. After 24 h, non-migrating cells were scraped off by a cotton swab. The cells on the lower surface of the membrane were fixed with methanol for 10 min and stained with 0.2 % crystal violet for 20 min. The migrated cells were shown by an inverted microscope and the number of migrated cells was counted per field.

Cell Invasion Assay

Cells were grown in RPMI supplemented with 10 % FBS. Matrigel (Trevigen, Inc. USA) was thawed overnight at 4 °C and kept on ice. Matrigel diluted in ice-cold, serum-free media with a final concentration of 3–5 mg/ml. 100-μl matrigel was added into the upper compartment of the transwell chambers (6.5-mm diameter insert, 8.0-μm pore size; BD Biosciences, San Jose,

CA, USA) and incubated at 37 °C for 2 h to polymerize the matrigel. Cells were trypsinized and washed two times with serum-free media and re suspended in RPMI at 5×10^4 cells/ml. 600 μl of RPMI supplemented with 10 % FBS as attractant were added into the lower compartment of transwell chamber. The cells were added to the upper part of the chamber. The plate was incubated at the 37 °C for 24 h and the rest of the experiment was done as described in migration analysis.

Results

Epitope Designing by In silico Techniques

Simulated protein models (Fig. 1) were evaluated using SAVES program and our modeled molecules had proper structures based on the program parameters such as Ramachandran plot. Protein–protein interaction between Wnt-5a and CD146 was done by Hex 8.0.0 program (Fig. 2), the best docking result was obtained with Etotal, −854.66 kJ/mol, Eshape, −969.15 kJ/mol, and Eforce, 114.48 Kcal/mol. Evaluating the orientation of two molecules to one another using Chimera, showed that Wnt-5a binds to region of CD146 containing 70 amino acids from residue 250 to 320. These 70 amino acids were submitted in EpiC program and among the output sequences, based upon amino acid properties such as hydrophilicity, solvent accessibility, flexibility, and antigenicity, a 10 amino acid sequence (LADGNPPPHF) was selected for next experimental studies.

PCR and Fingerprinting

After 4 rounds of panning, 15 positive clones with scFv gene insert (Fig. 3) were selected and DNA fingerprint was done on these 15 colony PCR products. The dominant patterns were 6 out of 15 in the examined clones panned against the peptide (Fig. 4). This selected clone (IR94) was evaluated and used in the next steps.

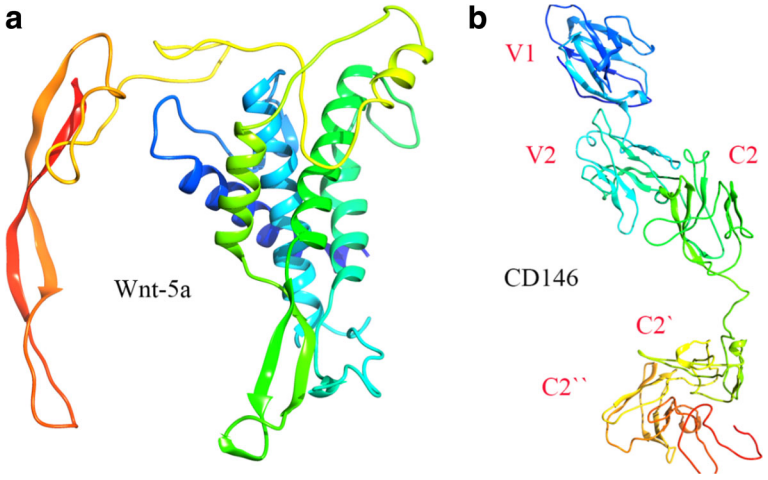

Fig. 1 Cartoon style of **a** Wnt-5a protein and **b** CD146 a multi-domain Ig-like receptor, it contains two variable domains (V1 and V2) and three constant domains (C2, C2, and C2)

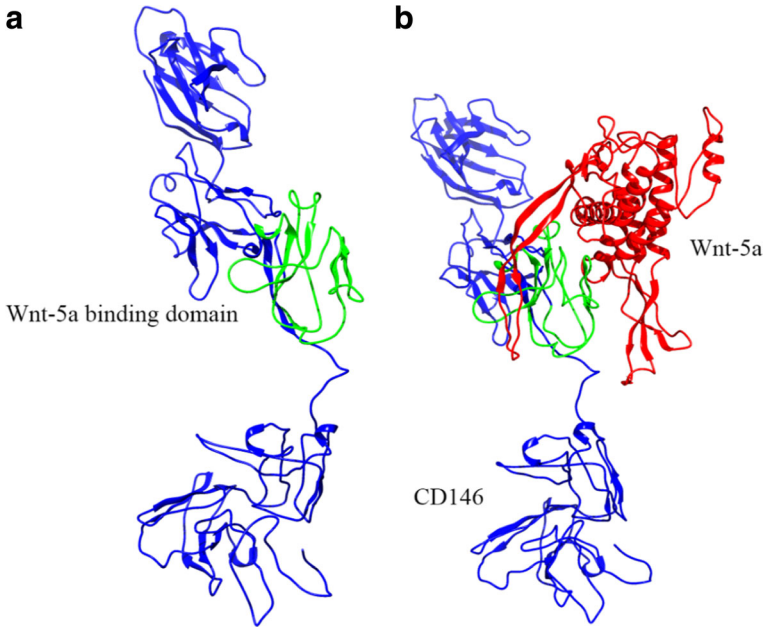

Fig. 2 Cartoon scene of **a** CD146 receptor containing 70 amino acid region (*green color*) for binding the Wnt-5a ligand and **b** binding of Wnt-5a molecule (*red color*) to the CD146 receptor (*blue color*)

Enzyme-Linked Immunosorbent Assay

To assess the affinity of the selected phage scFv (IR94) to the MUC18 epitope, the phage ELISA procedure was done. The anti-MUC18 phage scFv demonstrated specific and significant ELISA binding capacity to its peptide antigen. As shown in Fig. 5, at OD 450 nm, the mean absorbance of the reaction of anti-MUC18 scFv to the corresponding peptide was 1.4 while the mean absorbance of the reaction of this antibody to unrelated peptide and no peptide were 0.08 and 0.42, respectively. The mean absorbance obtained from the interaction of unrelated phage to the corresponding peptide was 0.3 (Fig. 5). *P* value between related peptide results and controls was <0.01, significantly.

Flow Cytometry

Flow cytometry was done to evaluate the cell binding property of anti-MUC18 phage scFv (IR94) to MDA-MB231 as positive cell line and SKBR3 as the negative cell line. The selected phage scFv showed 47.6 % fluorescence intensity for MDA-MB231 while this intensity was 5.33 % for SKBR3 cell line (Fig. 6a, b).

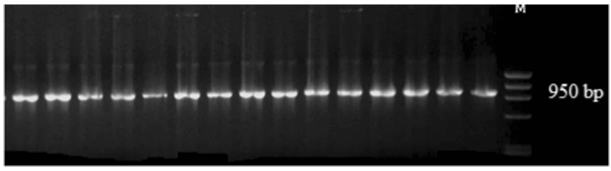

Fig. 3 PCR results related to scFv gene inserts. M is X174 DNA Marker

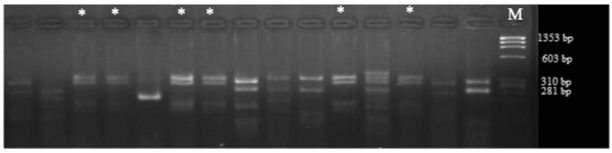

Fig. 4 DNA fingerprinting test. Patterns that marked by stars are same and dominant. The frequency of dominant patterns is 40 %. M is X174 DNA Marker

Expression of Soluble scFv

Expressed scFvs into the periplasmic space were solubilized and released to media supernatant. The supernatants of cell extracts were used as the soluble periplasmic fraction. One hundred microgram per milliliter of protein obtained from the periplasmic component of *HB2151* bacteria. The presence of 28 KD protein band on SDS-PAGE and Western blot indicated the isolated scFv (Fig. 6c).

Wound Healing Assay

Due to the high capacity of the MDA-MB231 cell line for the migration, after 8 h the artificial wound was healed in untreated plate (Fig. 7). The area of wounds in capturing photos based on the square of pixels was measured using digimizer software. As shown in Fig. 8, after 8 h, the artificial wound almost 98 % healed for untreated plate but for treated sample, the selected scFv (IR94) inhibited the movement of cells across the scratched gap (*P* value <0.0001).

Cell Migration and Invasion Assay

The metastasis potential of MDA-MB231, one of the common metastatic breast cancer cell lines, and the inhibitory effect of isolated anti-MUC18 scFv on it were evaluated. As shown in Fig. 9, the anti-MUC18 scFv reduced 76 % of the cell migration property (*P* value 0.002). The inhibitory effect for invasion assay was a 67 % reduction in cell invasiveness property (*P* value 0.009).

Discussion

Metastasis is a complex process in which cancer cells obtain some properties such as migration, invasion, and proliferation ability and lose some ability such as adhesion property [19]. MUC18 is expressed mostly on metastatic tumor cells and is only rarely detected in benign tumors [15]. Most evidences indicated that MUC18 could be a suitable antigen for targeted therapy, especially in clinically aggressive TNBC. The most lethal form of breast

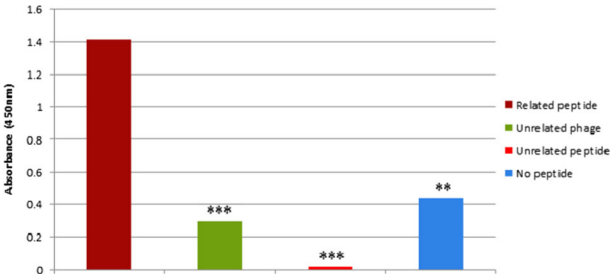

Fig. 5 ELISA results. The difference between the absorbance of anti-MUC18 phage scFv and negative controls were significant. $^{**}p < 0.01$ and $^{***}p < 0.001$ are based on the Student's *t* test

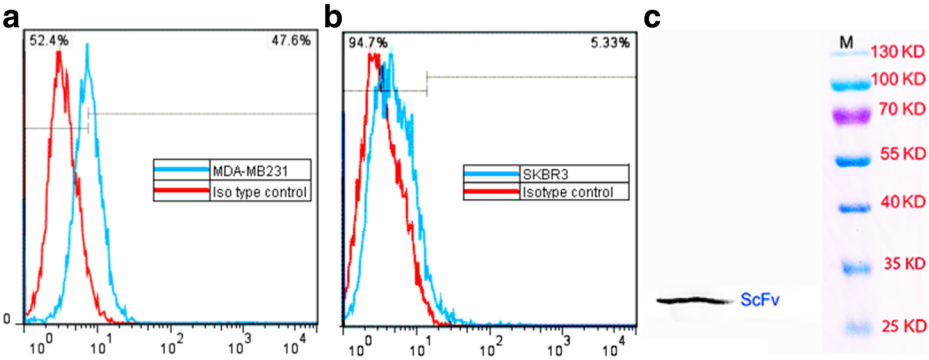

Fig. 6 Cell binding analysis results obtained by flow cytometry assay for **a** MDA-MB231 (positive cell line) and **b** SKBR3 (negative cell line). **c** Western blot test for 28 KD soluble anti-MUC18 scFv (IR94)

cancer is TNBC because it has a high incidence of resistance to current targeted therapies and the high tendency to metastasis [2, 34]. Recently, Witze et al. explained a mechanism of cell migration and invasion into which interaction between MUC18 and Wnt-5a molecules has a critical role [30]. Bioinformatic methods are appropriate tools to predict the structure and behavior of proteins [20]. In this study, using in silico methods such as molecular modeling and protein docking, we fabricated proper 3D models for MUC18 and Wnt-5a structures and evaluated the interaction between these two molecules to design the Wnt-5a binding site and the antigenic epitope on the MUC18 receptor. Molecular docking results showed that Wnt-5a can bind to C2 domain on the MUC18 receptor; we selected 70 amino acids from this region and searched for a suitable epitope based on its antigenicity, accessibility, and hydrophobicity. Based on mentioned criteria, a 10 amino acid length region was selected and used for downstream experimental studies. After selection and evaluation of scFv, we modeled the third structure of the anti-MUC18 scFv using homology modeling and found its binding region

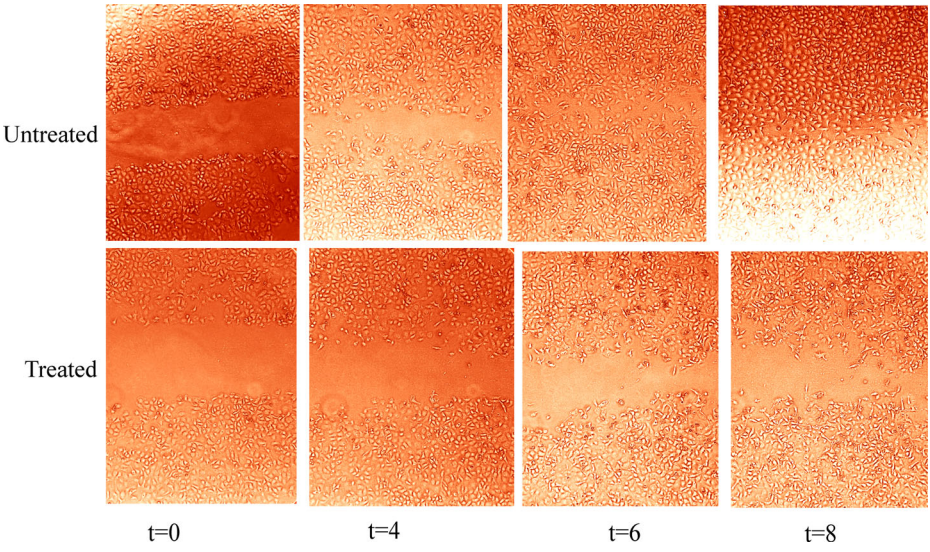

Fig. 7 Migration analysis of MDA-MB231 cell line treated with anti-MUC18 scFv compares to same cell line without scFv, by wound healing assay. Wound images captured at $t = 0$ h, $t = 4$ h, $t = 6$ h, and $t = 8$ h

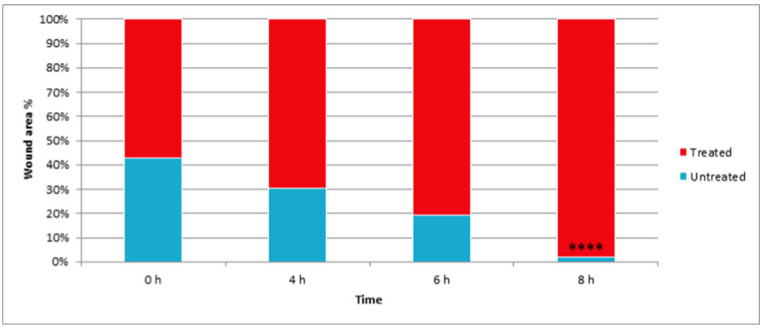

Fig. 8 Quantitative analysis of the wound healing assay. The wound area percent in the treated and untreated plates have been depicted by *different colors*. ****$p < 0.0001$ is based on the Student's t test between the treated and untreated plates

on MUC18 receptor by docking method (Fig. 10). Computational predictions have shown that anti-MUC18 scFv can compete with Wnt-5a for binding to the MUC18 receptor and acts as an antagonist agent.

In the experimental study, using the phage display method, we produced an anti-MUC18 scFv to prevent the aggressive behavior and metastases of TNBC breast cancer cells, such as MDA-MB231 which overexpresses the MUC18/CD146 [5]. Although scFv only has one VH and VL domain and lacks the rest components of the whole antibody, it retains the complete antigen binding properties and, in addition, the small size of scFvs enabled them for better penetration into solid-tumors [6]. The IR94 scFv showed reactivity for its epitope on the MUC18 antigen based on phage ELISA and flow cytometry results. In phage ELISA, the binding of the isolated phage scFv to the related peptide was 3.5 times greater than the no peptide control which indicates the significant positive reaction of phage scFv against the corresponding epitope. Moreover, assessing the cell binding capacity using flow cytometry showed that the selected phage scFv can bind to the corresponding antigen on MDA-MB231 cells almost 9-fold greater than SKBR3 cell line (as negative control).

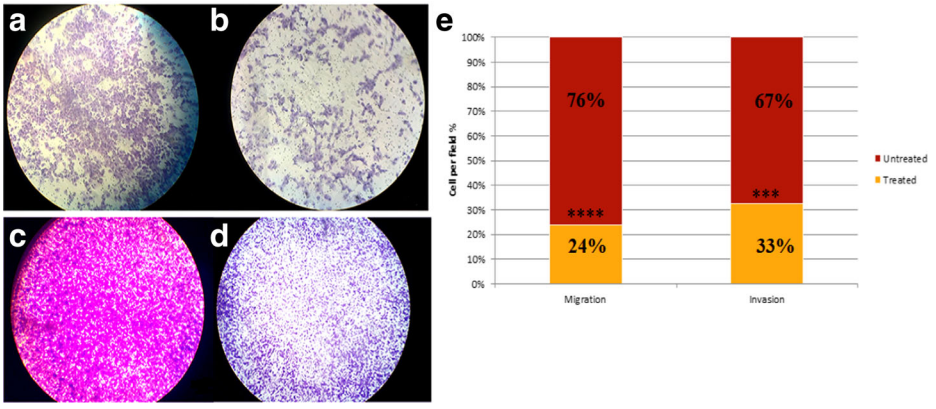

Fig. 9 **a**, **b** Treated and untreated MDA-MB231 cell line in migration test (400×). **c**, **d** Treated and untreated MDA-MB231 cell line in invasion assay (1000×). **e** Histogram exhibition of migration (*left*) and invasion (*right*) tests. The percent of migrated and invaded cells per field for treated and untreated states have been depicted by different colors. ***$p < 0.001$ and ****$p < 0.0001$ are based on the Student's t test between the treated and untreated samples

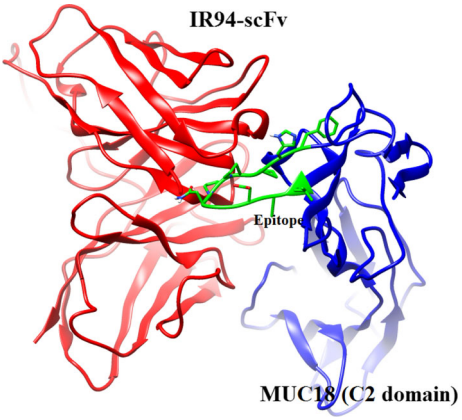

Fig. 10 Representative colored cartoon of anti-MUC18 scFv (IR94) binding to MUC18 receptor C2 domain

Isolated scFv was enabled to inhibit the migration (76 %) and invasion (67 %) of MUC18/CD146 positive cell line, MDA-MB231, significantly. Furthermore, for checking migration ability, wound healing or in vitro scratch assay was also used [29]. This method is almost similar to in vivo environment in fabricating migration [10]. The results of such assays could be extended to the pattern of migration in vivo [17]. As shown in Fig. 6, selected anti-MUC18 scFv was able to inhibit the movement of cells across the artificial scratch, whereas cells which were not treated with scFv antibody migrated and healed the wound. Keller and colleagues analyzed the binding of scFv-Fc B6-11 (an anti-MUC18 antibody) to blood endothelial cells (BECs) and inhibitory effects of it on migratory properties of these cells using the wound healing assay. In their study, scFv-Fc B6-11 could inhibit the gap closure almost 45 % in comparison with the control [12], while our scFv (IR94) prevented the artificial gap closure about 90 %. This difference might be due to applying the methods for selection of antigenic peptide. Unlike Keller et al., we explored and designed the epitope on MUC18 receptor with high accuracy by applying the bioinformatics methods.

As a result, the selected anti-MUC18 scFv, IR94 has the ability to interfere with breast cancer cell metastasis and invasion by disturbing the interaction between Wnt-5a and the MUC18 receptor. It may provide the more chance for other therapies to have better effect in the treatment of breast cancer, especially in TNBC format which does not respond to anti-HER2 monoclonal antibodies and hormonal therapy.

Acknowledgments This article was extracted from PhD thesis written by Mozafar Mohammadi, grant No 93-7365 and financially supported by Shiraz University of Medical Sciences, Shiraz, Iran.

Compliance with Ethical Standards

Conflicts of Interest None declared.

References

1. Structural analysis and verification server. http://nihserver.mbi.ucla.edu/SAVES (accessed on May 5th, 2014).
2. Andres, J. I., Alcazar, J., Alonso, J. M., Alvarez, R. M., Cid, J. M., De Lucas, A. I., Fernandez, J., Martinez, S., Nieto, C., Pastor, J., Bakker, M. H., Biesmans, I., Heylen, L. I., & Megens, A. A. (2003). Synthesis of 3a,

4-dihydro-3H-[1] benzopyrano [4,3-c] isoxazoles , displaying combined 5-HT uptake inhibiting and alpha (2)-adrenoceptor antagonistic activities: a novel series of potential antidepressants. *Bioorganic & Medicinal Chemistry Letters, 13*, 2719–2725.
3. Arnold, K., Bordoli, L., Kopp, J., & Schwede, T. (2006). The SWISS-MODEL workspace: a web-based environment for protein structure homology modelling. *Bioinformatics, 22*, 195–201.
4. Biasini, M., Bienert, S., Waterhouse, A., Arnold, K., Studer, G., Schmidt, T., Kiefer, F., Cassarino, T. G., Bertoni, M., Bordoli, L., & Schwede, T. (2014). SWISS-MODEL: modelling protein tertiary and quaternary structure using evolutionary information. *Nucleic Acids Research, 42*, W252–W258.
5. Chavez, K. J., Garimella, S. V., & Lipkowitz, S. (2010). Triple negative breast cancer cell lines: one tool in the search for better treatment of triple negative breast cancer. *Breast Disease, 32*, 35–48.
6. Deckert, P. M. (2009). Current constructs and targets in clinical development for antibody-based cancer therapy. *Current Drug Targets, 10*, 158–175.
7. Nejatollahi, F., Malek-Hosseini, Z., & Mehrabani, D. (2008). Development of single chain antibodies to P185 tumor antigen. *Iranian Red Crescent Medical Journal, 10*, 298–302.
8. Guex, N., Peitsch, M. C., & Schwede, T. (2009). Automated comparative protein structure modeling with SWISS-MODEL and Swiss-PdbViewer: a historical perspective. *Electrophoresis, 30*(Suppl 1), S162–S173.
9. Haslam, N. J., & Gibson, T. J. (2010). EpiC: an open resource for exploring epitopes to aid antibody-based experiments. *Journal of Proteome Research, 9*, 3759–3763.
10. Haudenschild, C. C., & Schwartz, S. M. (1979). Endothelial regeneration. II. Restitution of endothelial continuity. Laboratory investigation. *A Journal of Technical Methods and Pathology, 41*, 407–418.
11. Jemal, A., Bray, F., Center, M. M., Ferlay, J., Ward, E., & Forman, D. (2011). Global cancer statistics. *CA: a Cancer Journal for Clinicians, 61*, 69–90.
12. Keller, T., Kalt, R., Raab, I., Schachner, H., Mayrhofer, C., Kerjaschki, D., & Hantusch, B. (2015). Selection of scFv antibody fragments binding to human blood versus lymphatic endothelial surface antigens by direct cell phage display. *PloS One, 10*, e0127169.
13. Kelley, L. A., Mezulis, S., Yates, C. M., Wass, M. N., & Sternberg, M. J. (2015). The Phyre2 web portal for protein modeling, prediction and analysis. *Nature Protocols, 10*, 845–858.
14. Kiefer, F., Arnold, K., Kunzli, M., Bordoli, L., & Schwede, T. (2009). The SWISS-MODEL repository and associated resources. *Nucleic Acids Research, 37*, D387–D392.
15. Lehmann, J. M., Riethmuller, G., & Johnson, a J P. (1989). MUC18, a marker of tumor progression in human melanoma, shows sequence similarity to the neural cell adhesion molecules of the immunoglobulin superfamily. *Proceedings of the National Academy of Sciences of the United States of America, 86*(24), 9891–9895.
16. Lei, X., Guan, C. W., Song, Y., & Wang, H. (2015). The multifaceted role of CD146/MCAM in the promotion of melanoma progression. *Cancer Cell International, 15*, 3.
17. Liang, C. C., Park, A. Y., & Guan, J. L. (2007). In vitro scratch assay: a convenient and inexpensive method for analysis of cell migration in vitro. *Nature Protocols, 2*, 329–333.
18. Macindoe, G., Mavridis, L., Venkatraman, V., Devignes, M. D., & Ritchie, D. W. (2010). HexServer: an FFT-based protein docking server powered by graphics processors. *Nucleic Acids Research, 38*, W445–W449.
19. McSherry, E. A., Donatello, S., Hopkins, A. M., & McDonnell, S. (2007). Molecular basis of invasion in breast cancer. *Cellular and Molecular Life Sciences: CMLS, 64*, 3201–3218.
20. Mohammadi, M., & Nejatollahi, F. (2014). 3D structural modeling of neutralizing scFv against glycoprotein-D of HSV-1 and evaluation of antigen-antibody interactions by bioinformatic methods. *International Journal of Pharma and Bio Sciences, 5*(4), 835–847.
21. Monnier, P. P., Vigouroux, R. J., & Tassew, a N G. (2013). In vivo applications of single chain Fv (variable domain) (scFv) fragments. *Antibodies, 2*, 193–208.
22. Mostert, B., Sleijfer, S., Foekens, J. A., & Gratama, J. W. (2009). Circulating tumor cells (CTCs): detection methods and their clinical relevance in breast cancer. *Cancer Treatment Reviews, 35*, 463–474.
23. Nejatollahi, F., Asgharpour, M., & Jaberipour, M. (2012). Down-regulation of vascular endothelial growth factor expression by anti-Her2/neu single chain antibodies. *Medical Oncology, 29*, 378–383.
24. Nejatollahi, F., Ranjbar, R., Younesi, V., & Asgharpour, M. (2012). Deregulation of HER2 downstream signaling in breast cancer cells by a cocktail of anti-HER2 scFvs. *Oncology Research, 20*, 333–340(338).
25. Nejatollahi, F., Abdi, S., & Asgharpour, M. (2013). Antiproliferative and apoptotic effects of a specific antiprostate stem cell single chain antibody on human prostate cancer cells. *Journal of Oncology, 2013*, 839831.
26. Nejatollahi F, Jaberipour M, Asgharpour M (2014) Triple blockade of HER2 by a cocktail of anti-HER2 scFv antibodies induces high antiproliferative effects in breast cancer cells. Tumour biology : the journal of the International Society for Oncodevelopmental Biology and Medicine
27. Nelson, A. L. (2010). Antibody fragments: hope and hype. *MAbs, 2*, 77–83.
28. Pettersen, E. F., Goddard, T. D., Huang, C. C., Couch, G. S., Greenblatt, D. M., Meng, E. C., & Ferrin, T. E. (2004). UCSF chimera—a visualization system for exploratory research and analysis. *Journal of Computational Chemistry, 25*, 1605–1612.

29. Todaro, G. J., Lazar, G. K., & Green, H. (1965). The initiation of cell division in a contact-inhibited mammalian cell line. *Journal of Cellular Physiology, 66*, 325–333.
30. Witze, E. S., Connacher, M. K., Houel, S., Schwartz, M. P., Morphew, M. K., Reid, L., Sacks, D. B., Anseth, K. S., & Ahn, N. G. (2013). Wnt5a directs polarized calcium gradients by recruiting cortical endoplasmic reticulum to the cell trailing edge. *Developmental Cell, 26*, 645–657.
31. Wu, G.-J. (2012). MCAM (melanoma cell adhesion molecule). *Atlas of Genetics and Cytogenetics in Oncology Haematology, 16*, 7.
32. Wu, G. J., Wu, M. W., Wang, S. W., Liu, Z., Qu, P., Peng, Q., Yang, H., Varma, V. A., Sun, Q. C., Petros, J. A., Lim, S. D., & Amin, M. B. (2001). Isolation and characterization of the major form of human MUC18 cDNA gene and correlation of MUC18 over-expression in prostate cancer cell lines and tissues with malignant progression. *Gene, 279*, 17–31.
33. Ye, Z., Zhang, C., Tu, T., Sun, M., Liu, D., Lu, D., Feng, J., Yang, D., Liu, F., & Yan, X. (2013). Wnt5a uses CD146 as a receptor to regulate cell motility and convergent extension. *Nature Communications, 4*, 2803.
34. Zeng, Q., Li, W., Lu, D., Wu, Z., Duan, H., Luo, Y., Feng, J., Yang, D., Fu, L., & Yan, X. (2012). CD146, an epithelial-mesenchymal transition inducer, is associated with triple-negative breast cancer. *Proceedings of the National Academy of Sciences of the United States of America, 109*, 1127–1132.